Supporting Information

MATERIALS AND METHODS

Plasmid construction. The strains and plasmids used in this study are listed in Table S5. The primers used in this study are listed in Table S6. The integrity of all PCR-derived constructs was verified by sequencing. The plasmids pKH239, pKH241, and pKH274 are suicide vectors based on pRL277 (1) used to cleanly delete the coding regions of the genes *alr2902*, *alr3234*, and *asl1930*, respectively. Regions up- and down-stream of *alr2902*, *alr3234*, and *asl1930* were amplified by PCR from *Anabaena* chromosomal DNA with the primer pairs d2902-up-F and d2902-up-R and d2902-dn-F and d2902-dn-R, d3234-up-F and d3234-up-R and d3234-dn-F and d3234-dn-R, and 1930-up-F and 1930-up-R and 1930-dn-F and 1930-dn-R, respectively. The up- and downstream regions were fused together by overlap extension PCR (2) and individually cloned as *Blg*II-*Sac*I fragments into the same sites of pRL277.

The plasmids pPJAV298, pPJAV299, pPJAV300, pPJAV301, pPJAV302, pPJAV303, and pPJAV304 are mobilizable shuttle vectors based on pAM504 carrying seven alleles of *hetP* lacking a range of amino acids: Δ26-159, Δ51-159, Δ69-159, Δ76-159, Δ101-159, Δ126-159, and native length *hetP*, respectively, expressed by the *hetP* promoter. Fragments of the *hetP* coding region were amplified via PCR using *Anabaena* chromosomal DNA as a template. The upstream primer used to create these fragments was hetP-up-XhoI and the following downstream primers were used to make specific *hetP* alleles: hetP-25aa-EcoRV-R for pPJAV298; hetP-50aa-EcoRV-R for pPJAV299; hetP-68aa-EcoRV-R for pPJAV300; hetP-75aa-EcoRV-R for pPJAV301; hetP-100aa-EcoRV-R for pPJAV302; hetP-125aa-EcoRV-R for pPJAV303; and hetP-159aa-EcoRV-R for pPJAV304. The products were individually cloned as *Xho*I-*Eco*RV fragments into the *Sal*I-*Sma*I sites in pAM504 (3).

The plasmids pPJAV305, pPJAV306, and pPJAV307 are mobilizable shuttle vectors based on pAM504 carrying alleles of *hetP* encoding C36A, C95A, and C36A/C95A substitutions, respectively, expressed by the *hetP* promoter. The fragments used to make base substitutions were amplified via overlap extension PCR using *Anabaena* chromosomal DNA as a template. The outer primers used to create the constructs were hetP-up-XhoI and hetP-159aa-EcoRV-R. The following internal primer pairs were used to create specific *hetP* alleles: hetPC36A-F M475L and hetPC36A-R M475L for pPJAV305; hetPC95A-F M475L and hetPC95A-R M475L for pPJAV306; and, using pPJAV238 as a template, hetPC95A-F M475L and hetPC95A-R M475L for pPJAV307. These were cloned as *Xho*I-*Eco*RV fragments into the *Sal*I-*Sma*I sites in pAM504.

Plasmid pPJAV327 is a suicide vector based on pRL277 used to reintroduce the native *hetP* allele into the *hetP* locus. A fragment containing regions up- and down-stream of hetP as well as the hetP coding sequence were was amplified by PCR using *Anabaena* chromosomal DNA as a template with the primers del-hetP-up-F and del-hetP-up-R. This product was cloned into the *Nru*I site in pRL277.

The plasmids pPJAV330, pPJAV331, and pPJAV332 are mobilizable shuttle vectors based on pAM504 carrying transcriptional fusions with the promoters of *asl1930*, *alr2902*, and *alr3234* to *gfp*, respectively. The promoter regions of *asl1930*, *alr2902*, and

alr3234 were amplified by PCR using *Anabaena* chromosomal DNA as a template with the primer pairs Pasl1930-XhoI-F M475L and Pasl1930-R M475L, Palr2902-XhoI-F M475L and Palr2902-R M475L, and Palr3234-XhoI-F M475L and Palr3234-R M475L, respectively. The products were individually cloned into the *Sma*I site in pAM1956 and screened for directionality with PCR (4).

The plasmids pPJAV353, pPJAV354, and pPJAV358 are mobilizable shuttle vectors based on pAM504 carrying transcriptional fusions of the *hetP* promoter to 68 amino acid-long alleles of *asl1930, alr2902*, and *alr3234* that share homology with *hetP*. The fragments used to make base substitutions were amplified via overlap extension PCR using *Anabaena* chromosomal DNA as a template. The primers hetP-up-XhoI and PhetP-R were used to amplify the *hetP* promoter. The following primer pairs were used to amplify the desired alleles of *asl1930, alr2902*, and *alr3234*: asl1930-68aa-F and asl1930-68aa-R for pPJAV353; alr2902-68aa-F and alr2902-68aa-R for pPJAV354; and alr3234-68aa-F and alr3234-68aa-R for pPJAV358. The products were individually cloned into the *Sma*I site in pAM504 and screened for directionality with PCR to insure that all inserts transcribed in the same direction.

The plasmids pT18 C-link amp, pT18 N-link amp, pT25 C-link kan, and pT25 N-link kan are vectors created by the addition of nucleotides encoding an 11 amino acid linker (GSAGSAAGSGG) to pUT18C, pUT18, pKT25, and pKNT25, respectively (5). pT18 C-link amp was built by PCR amplifying the T18 region of pUT18C with the primers T18C-HindIII F and T18C-link-PstI R. The product was cloned as a *Hind*III-*Pst*I fragment into the same sites of pUT18C. pT18 N-link amp was built by PCR amplifying the T18 region of pUT18 with the primers T18N-link-EcoRI F and T18N-EagI R. The product was cloned as an *EcoR*I-*Eag*I fragment into the same sites of pUT18. pT25 C-link kan was built by PCR amplifying the T25 region of pKT25 with the primers T25C-HindIII F and T25C-link-PstI R. The product was cloned as a *Hind*III-*Pst*I fragment into the same sites of pKT25. pT25 N-link kan was built by PCR amplifying the T25 region of pKNT25 with the primers T25N-NheI F and T25N-link-EcoRI. The product was cloned as a *Nhe*I-*EcoR*I fragment into the same sites of pKNT25 to create the plasmids pT18 C-link amp, pT18 N-link amp, pT25 C-link kan, and pT25 N-link kan, respectively.

The plasmids pRO176, pRO180, pRO184, and pRO188 are vectors based on pT18-C-link carrying C-terminal translational fusions of *hetP, asl1930, alr2902*, and *alr3234*, respectively, with the T18 *cyaA* domain. The coding regions of *hetP, asl1930, alr2902*, and *alr3234* were amplified from *Anabaena* chromosomal DNA with the primer pairs Bac2-C-hetP XbaI F and Bac2-C-hetP KpnI R, Bac2-C-asl1930 XbaI F and Bac2-C-asl1930 KpnI R, Bac2-C-alr2902 XbaI F and Bac2-C-alr2902 KpnI R, and Bac2-C-alr3234 XbaI F and Bac2-C-alr3234 KpnI R, respectively. The products were cloned as *Xba*I-*Kpn*I fragments into the same sites in pT18-C-link to create pRO176, pRO180, pRO184, and pRO188.

The plasmids pRO177, pRO181, pRO185, and pRO189 are vectors based on pT18-N-link carrying N-terminal translational fusions of *hetP, asl1930, alr2902*, and *alr3234*, respectively, with the T18 *cyaA* domain. The coding regions of *hetP, asl1930, alr2902*, and *alr3234* were amplified from *Anabaena* chromosomal DNA with the primer pairs Bac2-N-hetP XbaI F and Bac2-N-hetP KpnI R, Bac2-N-asl1930 XbaI F and Bac2-N-asl1930 KpnI R, Bac2-N-alr2902 XbaI F and Bac2-N-alr2902 KpnI R, and Bac2-N-alr3234 XbaI F and Bac2-N-alr3234 KpnI R, respectively. The products were cloned as

*Xba*I-*Kpn*I fragments into the same sites in pT18-N-link to create pRO177, pRO181, pRO185, and pRO189.

The plasmids pRO178, pRO182, pRO186, and pRO190 are vectors based on pT25-C-link carrying C-terminal translational fusions of *hetP*, *asl1930*, *alr2902*, and *alr3234*, respectively, with the T25 *cyaA* domain. The coding regions of *hetP*, *asl1930*, *alr2902*, and *alr3234* were amplified from *Anabaena* chromosomal DNA with the primer pairs Bac2-C-hetP XbaI F and Bac2-C-hetP KpnI R, Bac2-C-asl1930 XbaI F and Bac2-C-asl1930 KpnI R, Bac2-C-alr2902 XbaI F and Bac2-C-alr2902 KpnI R, and Bac2-C-alr3234 XbaI F and Bac2-C-alr3234 KpnI R, respectively. The products were cloned as *Xba*I-*Kpn*I fragments into the same sites in pT25-C-link to create pRO178, pRO182, pRO186, and pRO190.

The plasmids pRO179, pRO183, pRO187, and pRO191 are vectors based on pT25-N-link carrying N-terminal translational fusions of *hetP*, *asl1930*, *alr2902*, and *alr3234*, respectively, with the T25 *cyaA* domain. The coding regions of *hetP*, *asl1930*, *alr2902*, and *alr3234* were amplified from *Anabaena* chromosomal DNA with the primer pairs Bac2-N-hetP XbaI F and Bac2-N-hetP KpnI R, Bac2-N-asl1930 XbaI F and Bac2-N-asl1930 KpnI R, Bac2-N-alr2902 XbaI F and Bac2-N-alr2902 KpnI R, and Bac2-N-alr3234 XbaI F and Bac2-N-alr3234 KpnI R, respectively. The products were cloned as *Xba*I-*Kpn*I fragments into the same sites in pT25-N-link to create pRO179, pRO183, pRO187, and pRO191.

Strain construction. All *Anabaena* strains used in this study are listed in Table S4. Clean, unmarked deletions of the *asl1930*, *alr2902*, and *alr3234* genes were introduced into either the wild type or UHM158, or resulting derivatives, using the plasmids pKH239, pKH241, or pKH274, respectively, in the order listed. To create UHM342, the *hetP* gene was reintroduced into the native locus in strain UHM333 using plasmid pPJAV327. Mutant strains were created as previously described (6-8). To confirm the mutant constructions, primers flanking the mutation and located outside the region of *Anabaena* DNA used to make the mutations were used to amplify the region of the intended mutation. The resulting sizes of the PCR products, as well as sensitivity to spectinomycin and streptomycin, were used to confirm that the desired deletions had been introduced. The primer pairs used to confirm deletion of the *hetP*, *asl1930*, *alr2902*, and *alr3234* genes were del-hetP-up-out and del-hetP-dn-out, 1930-up-out and 1930-dn-out, 2902-up-out and 2902-dn-out, and 3234-up-out and 3234-dn-out, respectively.

Replacement of the coding region of *patS* with an Ω interposon that confers resistance to spectinomycin and streptomycin in UHM158 with the plasmid pSMC164 was accomplished by allelic exchange as described above. Strain UHM334 with mutations in the *hetP* and *patS* genes was verified by PCR with the primer sets del-hetP-up-out and del-hetP-dn-out and patSfor and patSrev, respectively, which anneal outside of the regions used to make the deletions.

Alcian blue staining and acetylene reduction assays. Heterocyst-specific exopolysaccharide was stained with alcian blue as previously described (9, 10). Aerobic acetylene reduction assays were performed as previously described (11, 12).

Phylogenetic, structural, and statistical analyses. Amino acid sequences were aligned using the BLOSUM62 exchange weights matrix within the PRofile ALIgNEment (PRALINE) multiple sequence alignment application (13, 14). Phylogenetic analysis was performed using the Maximum Likelihood method based on the JTT matrix-based model

in MEGA6 (15, 16). The analysis included 17 amino acid sequences with 1000 bootstrap replicates. Tertiary structure prediction utilized the RaptorX software (17).

To mathematically assess epistasis, the fitness of each mutant was determined by its ability to differentiate heterocysts compared to the levels produced by the wild type (18). After calculating fitness (the percentage of heterocysts produced divided by the corresponding value for the wild type), epistasis (*e*) was calculated using a published two-allele two-phenotype equation ($e = \ln_{AB} \times \ln_{ab} - \ln_{aB} \times \ln_{Ab}$) in which the fitness values obtained for each strain are represented by *AB* (wild type), *Ab* (mutant for one gene), *aB* (mutant for the other gene), *ab* (the double mutant) because the interaction of only two loci was compared in any given treatment (19). Multiple regression analysis was performed using the R statistical package (20).

Pixel intensity measurement of images. Pixel intensity was measured using Adobe Photoshop by sampling 10-pixel diameter regions of interest from either the interior of 10 contiguous cells or 10 adjacent points in the background. The green channel pixel intensities were averaged, standard deviation was calculated, and significance assessed by *t*-test.

Heterocyst commitment assays. *Anabaena* strains were grown on solid BG-11 media supplemented with 5 mM ammonia for 48 hours and then transferred to 100 ml of liquid BG-11 media supplemented with 6 mM ammonia and grown under standard growth conditions for 24 hours. Heterocyst development was induced by washing each culture 3 times with BG-11_0 media, which lacks a combined nitrogen source. Washed cells were resuspended in 100 ml of BG-11_0 and grown under standard growth conditions for the remainder of the experiment. To test for commitment, a 2 ml sample was removed from the parent culture and transferred to a culture tube and ammonia was added to a final concentration of 6 mM at the time points indicated. Heterocyst development was assessed 24-48 hours later by counting morphologically distinct heterocysts. Percentages were calculated as the number of morphologically distinct heterocyst cells per 500 cells total. All results are the average of 3 replicates. Error bars represent the standard deviation.

Bacterial two-hybrid assays and β-galactosidase assays. Bacterial two-hybrid assays were performed as described (21, 22). Plasmids were introduced into competent DHM1 cells and transformants were selected on plates supplemented with ampicillin and kanamycin. Following overnight growth, single-colony transformants were inoculated into 2 ml LB cultures and incubated at 37°C with shaking. Cultures were grown to OD_{600} ~1.6 and 10 µl was spot inoculated onto LB plates supplemented with 40 µg/ml X-gal, 1 mM IPTG, ampicillin, and kanamycin and incubated for 18 h at 30°C. β-galactosidase activity was visually assessed and all assays were photodocumented. LB cultures for quantitative bacterial two-hybrid assays were grown to mid-log-phase (OD_{600} ~ 0.5) at 37°C with shaking and one ml was harvested and resuspended in an equal volume of Z-buffer. β-galactosidase activity was quantified as previously described and is presented as the average of three independent cultures (23). Error bars represent the standard deviation.

RNA isolation and first strand cDNA synthesis. Cells were grown in BG-11 media supplemented with ammonia and stepped down to media lacking combined nitrogen as previously described (24). Duplicate samples of approximately 2 million cells were harvested at times 0, 6, 12, 18, or 24 hours after stepdown. Cell pellets were

resuspended in 1ml of TRIzol reagent. Using a Misonex S-4000 probe sonicator, each sample was sonicated at 15% for 20 seconds for four pulses with 3 min on ice between each pulse. After addition of chloroform to the TRIzol mixture, the organic phase was transferred to Qiagen RNAeasy columns and the RNA was purified according to manufacturer's instructions. Total RNA was DNAseI treated on column for 30 min at room temperature. The RNA quality was evaluated with an Agilent RNA Tapestation on a R6K Screen tape. First strand cDNA synthesis was conducted using the SuperScriptIII System with random hexamers and varying amounts of RNA template (70-1500 ng) according to manufacturer's instructions.

RT-qPCR. Standard curves were generated to validate each target and housekeeping gene using eight 1:5 serial dilutions of *Anabaena* chromosomal DNA starting at 4 ng. Triplicate reactions were assembled manually and consisted of 1x LightCycler 480 SYBR Green I Master Mix, 0.5 μM of each forward/reverse primer pair (NrnpAF/NrnpAR, asl1930-qF/asl1930-qR, alr2902-qF/alr2902-qR, alr3234-qF/alr3234-qR, hetP-qF/hetP-qR) in a final reaction volume of 15 μL. The resulting standard curves show efficiencies for all primer sets between 91.0-94.5% ($r^2 > 0.998$). RT-qPCR reactions were assembled manually and contained 1x LightCycler 480 SYBR Green I Master Mix, 0.5 μM of each forward/reverse primer, and 0.6 μL of each cDNA reaction in a final volume of 15 μL. All standards and samples were run on a Roche LC480II using the following reaction profile: an initial denaturation at 95°C for 15 min, followed by 45 cycles of 95°C for 15 s, 60°C for 30 s, 72°C for 30 s, and a melting curve cycle of 65-95°C. Negative controls (no template cDNA) were included and a melting curve analysis was performed in all cases, which always yielded a single product. The relative quantities of each sample were calculated using the ΔΔCt method, taking into account each primer's specific efficiency calculated from the standard curves, as previously described (25). All values were normalized to *rnpA* expression because this gene was shown to be consistently expressed across growth conditions (26).

References cited

1. Black TA, Cai Y, & Wolk CP (1993) Spatial expression and autoregulation of *hetR*, a gene involved in the control of heterocyst development in *Anabaena*. *Mol. Microbiol.* 9:77-84.

2. Higuchi R, Krummel B, & Saiki RK (1988) A general method of *in vitro* preparation and specific mutagenesis of DNA fragments: study of protein and DNA interactions. *Nucleic Acids Res.* 16:7351-7367.

3. Wei T-F, Ramasubramanian R, & Golden JW (1994) *Anabaena* sp. strain PCC 7120 *ntcA* gene required for growth on nitrate and heterocyst development. *J. Bacteriol.* 176:4473-4482.

4. Yoon H-S & Golden JW (1998) Heterocyst pattern formation controlled by a diffusible peptide. *Science* 282:935-938.

5. Blair KM, Turner L, Winkelman JT, Berg HC, & Kearns DB (2008) A molecular clutch disables flagella in the *Bacillus subtilis* biofilm. *Science* 320(5883):1636-1638.

6. Cai Y & Wolk CP (1990) Use of a conditionally lethal gene in *Anabaena* sp. strain PCC 7120 to select for double recombinants and to entrap insertion sequences. *J. Bacteriol.* 172:3138-3145.

7. Callahan SM & Buikema WJ (2001) The role of HetN in maintenance of the heterocyst pattern in *Anabaena* sp. PCC 7120. *Mol. Microbiol.* 40:941-950.

8. Orozco CC, Risser DD, & Callahan SM (2006) Epistasis analysis of four genes from *Anabaena* sp. strain PCC 7120 suggests a connection between PatA and PatS in heterocyst pattern formation. *J. Bacteriol.* 188(5):1808-1816.

9. Higa KC & Callahan SM (2010) Ectopic expression of *hetP* can partially bypass the need for *hetR* in heterocyst differentiation by *Anabaena* sp strain PCC 7120. *Mol. Microbiol.* 77:562-574.

10. McManus JFA & Mowry RW (1960) *Staining Methods. Histologic and Histochemical* (Harper (Hoeber), New York) 1 Ed p 423.

11. Ernst A, *et al.* (1992) Synthesis of nitrogenase in mutants of the cyanobacterium *Anabaena* sp. strain PCC 7120 affected in heterocyst development or metabolism. *J. Bacteriol.* 174:6025-6032.

12. Videau P, *et al.* (2014) Expanding the direct HetR regulon in *Anabaena* sp. strain PCC 7120. *J. Bacteriol.* 196(5):1113-1121.

13. Simossis VA & Heringa J (2005) PRALINE: a multiple sequence alignment toolbox that integrates homology-extended and secondary structure information. *Nucleic Acids Res.* 33(Web Server issue):W289-W294.

14. Simossis VA, Kleinjung J, & Heringa J (2005) Homology-extended sequence aligenment. *Nucleic Acids Res.* 33(3):816-824.

15. Jones DT, Taylor WR, & Thorton JM (1992) The rapid generation of mutation data matrices from protein sequences. *Comput. Appl. Biosci.* 8:275-282.

16. Tamura K, Stecher G, Peterson D, Filiski A, & Kumar S (2013) MEGA6: Molecular evolutionary genetics analysis version 6.0. *Mol. Biol. Evol.* 30:2725-2729.

17. Källberg M, *et al.* (2012) Template-based protein structure modeling using the RaptorX web server. *Nat Protoc* 7(8):1511-1522.

18. Kouyos RD, Silander OK, & Bonhoeffer S (2007) Epistasis between deleterious mutations and the evolution of recombination. *Trends Ecol Evol* 22(6):308-315.

19. MacLean RC (2010) Predicting epistasis: an experimental test of metabolic control theory with bacterial transcription and translation. *J Evol Biol* 23(3):488-493.

20. Team RC (2013) R: A language and environment for statistical computingVienna, Austria).

21. Karimova G, Pidoux J, Ullmann A, & Ladant D (1998) A bacterial two-hybrid system based on a reconstituted signal transduction pathway. *Proc. Natl. Acad. Sci. USA* 95(10):5752-5756.

22. van den Ent F, *et al.* (2006) Dimeric structure of the cell shape protein MreC and its functional implications. *Mol Microbiol* 62(6):1631-1642.

23. Miller JH (1972) *Experiments in molecular genetics* (Cold Spring Harbor Laboratory, Cold Spring Harbor, N. Y.).

24. Borthakur PB, Orozco CC, Young-Robbins SS, Haselkorn R, & Callahan SM (2005) Inactivation of *patS* and *hetN* causes lethal levels of heterocyst differentiation in the filamentous cyanobacterium *Anabaena* sp. PCC 7120. *Mol. Microbiol.* 57:111-123.

25. Videau P, Wells KN, Singh AJ, Gerwick WH, & Philmus B (2016) Assessment of *Anabaena* sp. strain PCC 7120 as a heterologous expression host for cyanobacterial natural products: Production of lyngbyatoxin A. *ACS Synth. Biol.* 5(9):978-988.

26. Pinto F, Pacheco C, Ferreira D, Moradas-Ferreira P, & Tamagnini P (2012) Selection of suitable reference genes for RT-qPCR analyses in cyanobacteria. *PLoS One* 7(4):e34983.

Legends for Supplemental Figures

Figure S1. Vegetative cell interval lengths during *hetP* overexpression. Wild-type cells carrying either an empty P_{petE} vector (pPJAV213; black bars) or the copper-inducible P_{petE}-*hetP* (pSMC224; grey bars) were grown in nitrogen-replete conditions and stepped down to media lacking fixed nitrogen supplemented with 2 μM copper. After 24 hours, cells were imaged and the number of vegetative cells between heterocysts were counted for 300 intervals in each strain. The height of the bars (y-axis) represents the frequency of intervals with the indicated interval length (x-axis).

Figure S2. HetP is widely distributed and conserved. A) Phylogenetic tree generated by Maximum Likelihood method based on the JTT matrix-based model in MEGA6. Physiological characteristics associated with groupings are noted with brackets to the right. B) Amino acid sequences were aligned using the BLOSUM62 exchange weights matrix within the PRofile ALIgNEment (PRALINE) multiple sequence alignment application. Colors indicate degree of similarity from blue (no similarity) to red (identical). C) Sequence alignment of HetP (Alr2818), Asl1930, Alr2902, and Alr3234 of *Anabaena*. Colors indicate degree of conservation from blue (no similarity) to red (identical).

Figure S3. Bypass of wild type, *hetP*, *hetR*, and quadruple mutants by HetP and homologs. Average percent heterocysts out of 500 cells after nitrogen stepdown. Each background carries either an empty P_{petE} vector (pPJAV213), P_{petE}-*hetP* (pSMC224), P_{petE}-*asl1930* (pKH282), P_{petE}-*alr2902* (pKH281), or P_{petE}-*alr3234* (pSMC226). A) Δ*hetP* (UHM158) at 24 hours after stepdown. Strain Δ*hetR* (UHM103) 96 hours after nitrogen stepdown. B) Wild type 24 hours after stepdown. C) Quadruple mutant Δ*hetP* Δ*asl1930* Δ*alr2902* Δ*alr3234* (UHM333) 24 hours after stepdown. D) Quadruple mutant Δ*hetP* Δ*asl1930* Δ*alr2902* Δ*alr3234* (UHM333) 72 hours after stepdown. All media conditions were supplemented with copper to a final concentration of 2 μM. Error bars represent the standard deviation of the mean for 3 replicates.

Figure S4. Expression of P_{patS}-*gfp* in various *Anabaena* strains. Brightfield (BF), autofluorescence (AF), and GFP micrographs of wild type, Δ*hetP* Δ*asl1930* Δ*alr2902* (UHM282), Δ*hetP* Δ*asl1930* Δ*alr3234* (UHM283), Δ*hetP* Δ*alr2902* Δ*alr3234* (UHM284), and Δ*hetP* Δ*asl1930* Δ*alr2902* Δ*alr3234* (UHM333) carrying P_{patS}-*gfp* (pAM1951) 10 hours after nitrogen stepdown.

Figure S5. Expression of $P_{alr2902}$-*gfp* and $P_{alr3234}$-*gfp* in various *Anabaena* strains. Plasmids containing transcriptional fusions of the promoter regions of A) *alr2902* (pPJAV331) and B) *alr3234* (pPJAV332) to *gfp* were introduced into wild type (WT), Δ*hetR* (UHM103), Δ*patA* (UHM101), Δ*hetP* (UHM158), and Δ*hetP* Δ*asl1930* Δ*alr2902* Δ*alr3234* (UHM333). The resulting strains were grown in nitrogen-replete conditions and imaged (bright field, left columns and GFP, right columns). Strains were then stepped down to media lacking combined nitrogen and imaged after 24 hours (WT, Δ*hetR*, Δ*patA*) or 48 hours (Δ*hetP*, Δ*hetP* Δ*asl1930* Δ*alr2902* Δ*alr3234*). C) Relative expression of *hetP*, *alr2902*, and *alr3234* in the wild type measured by RT-qPCR at 6, 12, 18, and 24 hours after nitrogen stepdown. Height of the bars indicates the fold change in expression relative to time 0 for the same gene. Error bars represent the standard deviation. Asterisks indicate a significant difference in expression from time 0 ($p < 0.05$). D) Intensity of GFP signal from each GFP subpanel in part B. Average pixel intensity for cells (black bars) or background (grey bars) for each genotype indicated in either N+ or N- conditions. Error bars represent standard deviation. Each pair of bars is significantly different ($p < 0.001$).

Figure S6. Influence of HetR on gene expression. RNA was purified from Δ*hetR* (UHM103) and Δ*patA* (UHM101) strains at 0 hours and 24 hours after nitrogen

stepdown. RT-qPCR was performed using primer sets for A) *hetP*, B) *asl1930*, C) *alr2902*, and D) *alr3234*. Height of the bars indicates fold change in expression relative to wild type at the indicated time point (all bars $p < 0.05$). Error bars represent the standard deviation.

Figure S1

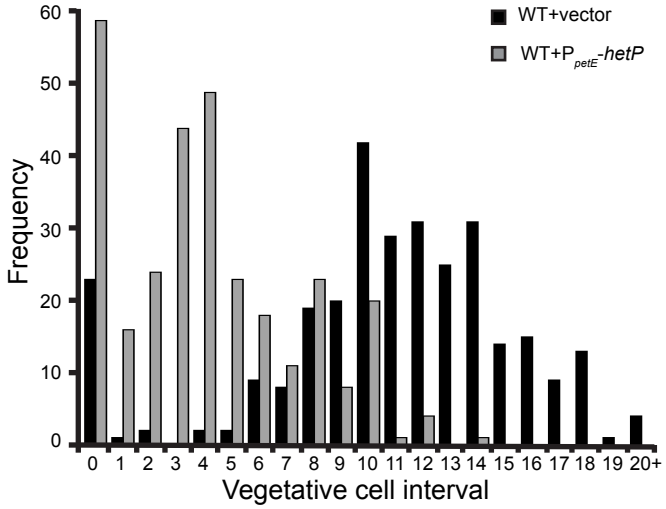
WT+vector
WT+P petE -hetP
Frequency
60
50
40
30
20
10
0
0 1 2 3 4 5 6 7 8 9 10 11 12 13 14 15 16 17 18 19 20+
Vegetative cell interval

Figure S2

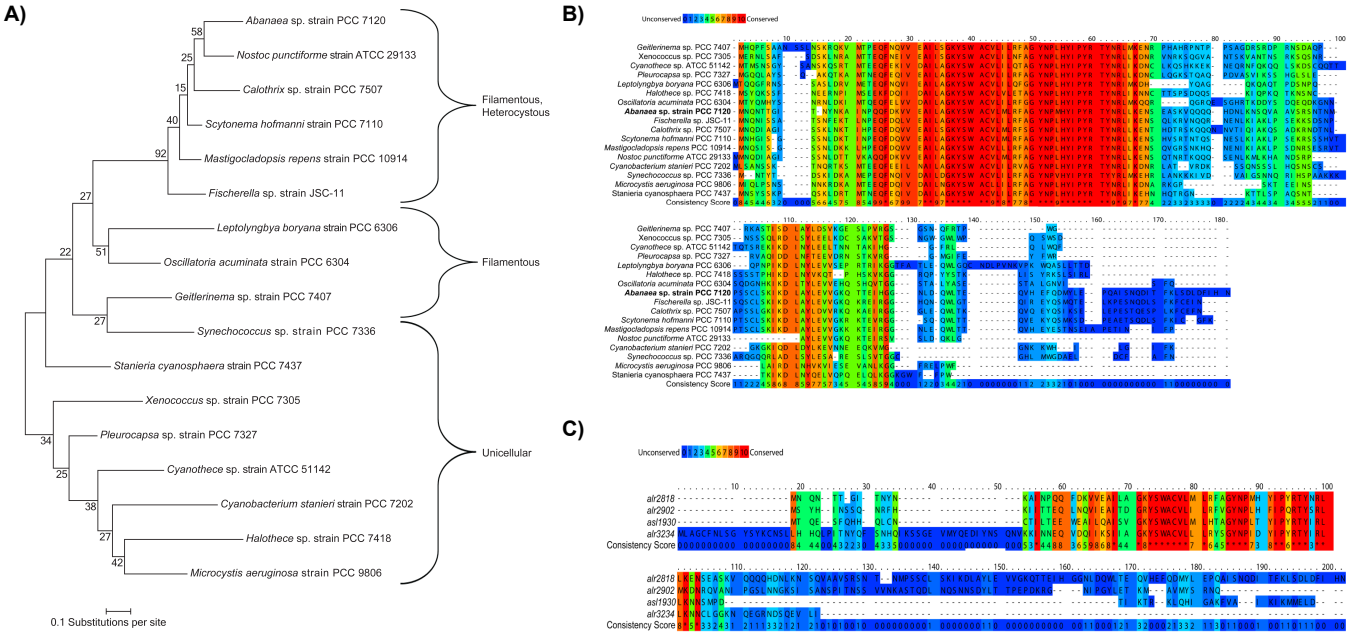
A)
Abanaea sp. strain PCC 7120
Nostoc punctiforme strain ATCC 29133
Calothrix sp. strain PCC 7507
Scytonema hofmanni strain PCC 7110
Mastigocladopsis repens strain PCC 10914
Fischerella sp. strain JSC-11
Filamentous, Heterocystous
Leptolyngbya boryana strain PCC 6306
Oscillatoria acuminata strain PCC 6304
Geitlerinema sp. strain PCC 7407
Synechococcus sp. strain PCC 7336
Filamentous
Stanieria cyanosphaera strain PCC 7437
Xenococcus sp. strain PCC 7305
Pleurocapsa sp. strain PCC 7327
Cyanothece sp. strain ATCC 51142
Cyanobacterium stanieri strain PCC 7202
Halothece sp. strain PCC 7418
Microcystis aeruginosa strain PCC 9806
Unicellular
0.1 Substitutions per site
B)
C)

Figure S3

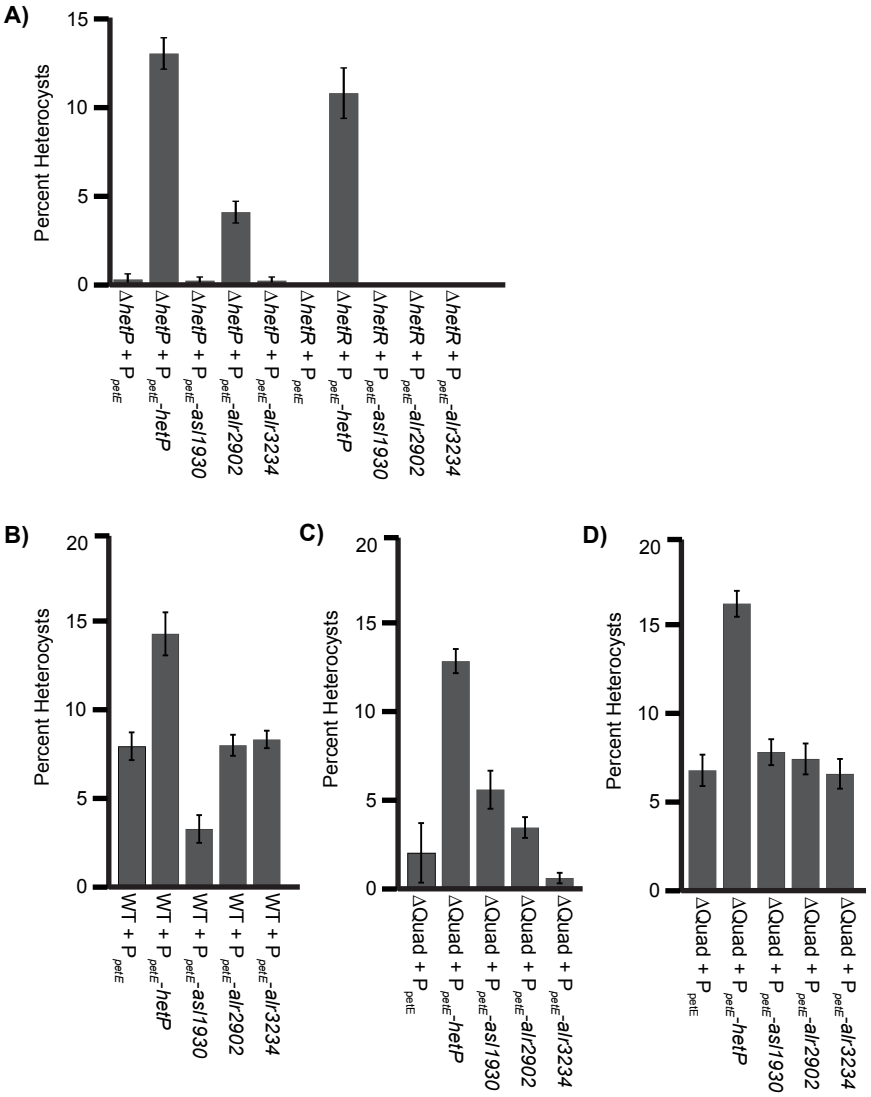
A)
Percent Heterocysts
15
10
5
0
ΔhetP + P petE
ΔhetP + P petE-hetP
ΔhetP + P petE-asl1930
ΔhetP + P petE-alr2902
ΔhetP + P petE-alr3234
ΔhetR + P petE
ΔhetR + P petE-hetP
ΔhetR + P petE-asl1930
ΔhetR + P petE-alr2902
ΔhetR + P petE-alr3234
B)
Percent Heterocysts
20
15
10
5
0
WT + P petE
WT + P petE-hetP
WT + P petE-asl1930
WT + P petE-alr2902
WT + P petE-alr3234
C)
Percent Heterocysts
20
15
10
5
0
ΔQuad + P petE
ΔQuad + P petE-hetP
ΔQuad + P petE-asl1930
ΔQuad + P petE-alr2902
ΔQuad + P petE-alr3234
D)
Percent Heterocysts
20
15
10
5
0
ΔQuad + P petE
ΔQuad + P petE-hetP
ΔQuad + P petE-asl1930
ΔQuad + P petE-alr2902
ΔQuad + P petE-alr3234

Figure S4

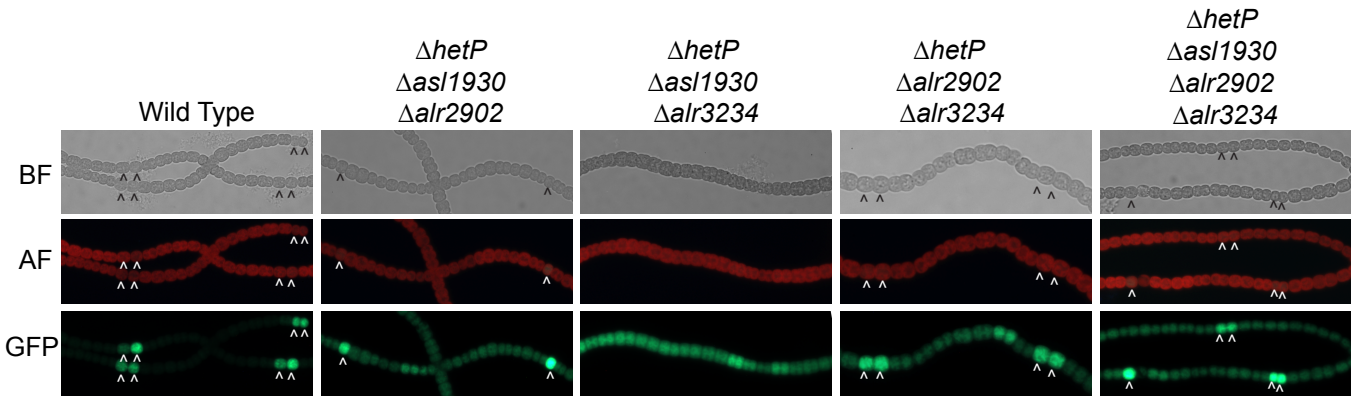
Wild Type
ΔhetP Δasl1930 Δalr2902
ΔhetP Δasl1930 Δalr3234
ΔhetP Δalr2902 Δalr3234
ΔhetP Δasl1930 Δalr2902 Δalr3234
BF
AF
GFP

Figure S5

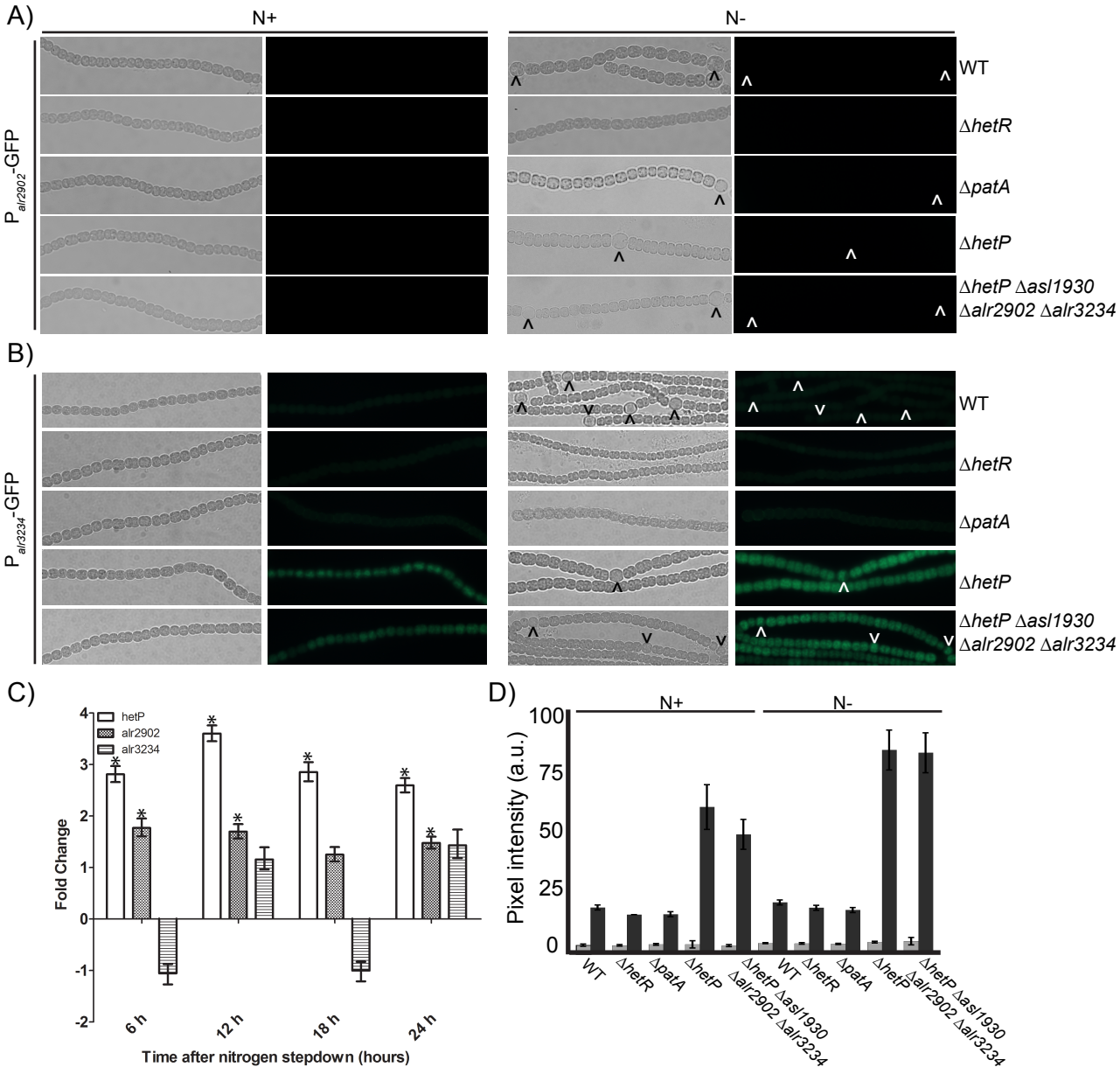
A)
N+
N-
$P_{alr2902}$-GFP
WT
ΔhetR
ΔpatA
ΔhetP
ΔhetP Δasl1930
Δalr2902 Δalr3234
B)
$P_{alr3234}$-GFP
WT
ΔhetR
ΔpatA
ΔhetP
ΔhetP Δasl1930
Δalr2902 Δalr3234
C)
hetP
alr2902
alr3234
Fold Change
6 h
12 h
18 h
24 h
Time after nitrogen stepdown (hours)
D)
N+
N-
Pixel intensity (a.u.)
WT
ΔhetR
ΔpatA
ΔhetP
ΔhetP Δasl1930 Δalr2902 Δalr3234
WT
ΔhetR
ΔpatA
ΔhetP
ΔhetP Δasl1930 Δalr2902 Δalr3234

Figure S6

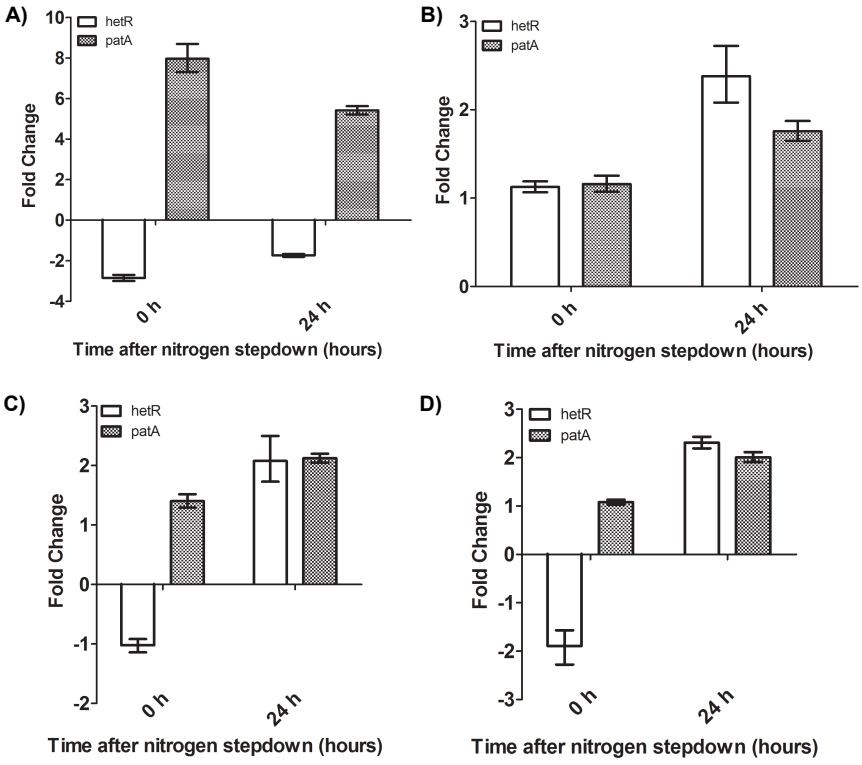
A)
hetR
patA
Fold Change
10
8
6
4
2
0
-2
-4
0 h
24 h
Time after nitrogen stepdown (hours)
B)
hetR
patA
Fold Change
3
2
1
0
0 h
24 h
Time after nitrogen stepdown (hours)
C)
hetR
patA
Fold Change
3
2
1
0
-1
-2
0 h
24 h
Time after nitrogen stepdown (hours)
D)
hetR
patA
Fold Change
3
2
1
0
-1
-2
-3
0 h
24 h
Time after nitrogen stepdown (hours)

Table S1. Patterns of heterocyst production and function by strains of *Anabaena*.

Strain	**Heterocyst Production (%)**	**Nitrogenase Activity (nmol C_2H_2/A_{750}*h)**	**Time of Commitment (h)**
Wild type	24h: 9.1 ± 0.6 48h: 7.31± 0.6 72h: 9.1 ± 0.4 96h: 8.7 ± 1.0 120h: 8.9 ± 0.3	0.705 ± 0.013	9-13
Δ*hetR* (UHM103)	24h: 0 48h: 0 72h: 0 96h: 0 120h: 0	0	N/A
Δ*patS*::Ω Sp^r/Sm^r (UHM334)	24h: 24.9 ± 2.7 48h: 20.1 ± 1.1 72h: 17.5 ± 1.9 96h: 15.7 ± 2.1 120h: 16.6 ± 1.3	0.323 ± 0.093	7-12
Δ*hetP* (UHM158)	24h: 0.4 ± 0.2 48h: 2.7 ± 0.5 72h: 3.0 ± 0.5 96h: 2.6 ± 0.9 120h: 3.1 ± 0.8	0.051 ± 0.005	20-36
Δ*hetP*Δ*patS*::Ω Sp^r/Sm^r (UHM223)	24h: 17.8 ± 0.7 48h: 12.9 ± 1.6 72h: 9.3 ± 0.8 96h: 9.4 ± 1.7 120h: 10.6 ± 1.1	0.243 ± 0.048	18-24
Δ*asl1930* (UHM295)	24h: 7.1 ± 0.4 48h: 7.6 ± 0.6 72h: 8.2 ± 0.5 96h: 7.7 ± 0.9 120h: 7.6 ± 0.7	0.222 ± 0.025	4-8
Δ*alr2902* (UHM296)	24h: 7.1 ± 0.4 48h: 8.4 ± 0.7 72h: 8.3 ± 0.8 96h: 8.0 ± 0.7 120h: 7.9 ± 1.2	0.376 ± 0.169	8-12
Δ*alr3234* (UHM336)	24h: 7.2 ± 1.2 48h: 7.5 ± 1.0 72h: 7.2 ± 0.3 96h: 7.0 ± 0.7 120h: 7.3 ± 1.0	0.479 ± 0.178	3-8
Δ*hetP*Δ*asl1930* (UHM288)	24h: 1.3 ± 0.6 48h: 1.4 ± 0.4	0.019 ± 0.003	N/D

	72h: 2.0 ± 0.5 96h: 2.0 ± 0.4 120h: 2.4 ± 0.5		
Δ*hetP*Δ*alr2902* (UHM287)	24h: 0 48h: 1.4 ± 0.6 72h: 2.4 ± 0.5 96h: 2.3 ± 0.6 120h: 2.2 ± 0.2	0.415 ± 0.046	N/D
Δ*hetP*Δ*alr3234* (UHM286)	24h: 0.2 ± 0.2 48h: 1.5 ± 0.3 72h: 2.0 ± 0.7 96h: 2.3 ± 0.6 120h: 2.5 ± 0.8	0.041 ± 0.018	N/D
Δ*asl1930*Δ*alr2902* (UHM297)	24h: 8.5 ± 0.5 48h: 8.5 ± 0.6 72h: 8.7 ± 0.6 96h: 8.4 ± 0.8 120h: 8.0 ± 0.6	0.916 ± 0.160	N/D
Δ*asl1930*Δ*alr3234* (UHM341)	24h: 8.5 ± 1.1 48h: 8.5 ± 0.9 72h: 8.0 ± 0.9 96h: 7.1 ± 0.6 120h: 7.5 ± 0.7	1.215 ± 0.249	N/D
Δ*alr2902*Δ*alr3234* (UHM343)	24h: 7.6 ± 0.5 48h: 9.0 ± 0.5 72h: 9.3 ± 0.5 96h: 8.3 ± 0.6 120h: 8.9 ± 1.0	0.789 ± 0.238	N/D
Δ*hetP*Δ*asl1930*Δ*alr2902* (UHM282)	24h: 1.1 ± 0.5 48h: 5.9 ± 0.9 72h: 6.9 ± 1.2 96h: 7.7 ± 1.0 120h: 7.3 ± 0.5	0.363 ± 0.062	N/D
Δ*hetP*Δ*asl1930*Δ*alr3234* (UHM283)	24h: 0 48h: 0 72h: 0 96h: 0 120h: 0	0	N/A
Δ*hetP*Δ*alr2902*Δ*alr3234* (UHM284)	24h: 1.2 ± 0.8 48h: 5.7 ± 0.7 72h: 7.1 ± 0.8 96h: 7.4 ± 0.5 120h: 7.4 ± 0.7	0.250 ± 0.048	N/D
Δ*asl1930*Δ*alr2902*Δ*alr3234* (UHM342)	24h: 9.9 ± 0.6 48h: 11.5 ± 0.6 72h: 11.3 ± 0.9	0	8-12

	96h: 11.5 ± 1.2 120h: 11.3 ± 0.7		
Δ*hetP*Δ*asl1930*Δ*alr2902*Δ*alr3234* (UHM333)	24h: 2.3 ± 0.5 48h: 5.2 ± 0.7 72h: 6.9 ± 0.8 96h: 7.3 ± 0.5 120h: 7.4 ± 0.5	0.332 ± 0.158	18-24

At the indicated times following nitrogen stepdown, 500 cells were counted in triplicate and total heterocysts are presented as the mean ± the standard deviation. Aerobic acetylene reduction assays were conducted in triplicate at 24 or 72 h (UHM158, UHM282, UHM283, UHM284, UHM286, UHM287, UHM288, and UHM233) after the removal of combined nitrogen and are presented as the mean ± the standard deviation. The time of commitment was defined as the duration required to transition from no heterocysts forming after the replacement of a nitrogen source to the maximum heterocyst percentage produced for the strain. N/D; not done. N/A; not applicable because the strain produced no heterocysts.

Table S2. Quantitative epistatic interactions govern heterocyst differentiation in strains mutant for *hetP*, *asl1930*, *alr2902*, and/or *alr3234*.

	Interaction between two loci			
	hetP	*asl1930*	*alr2902*	*alr3234*
hetP		-0.43	-0.18	-0.38
asl1930			0.16	0.14
alr2902				0.10
alr3234				
	Interaction between three loci			
	hetP	*asl1930*	*alr2902*	*alr3234*
hetP asl1930			1.28	N/A
hetP alr2902		1.02		1.12
hetP alr3234		N/A	1.32	
asl1930 alr2902	0.69			0.17
asl1930 alr3234	N/A		0.20	
alr2902 alr3234	0.84	0.23		
	Interaction between four loci			
	hetP	*asl1930*	*alr2902*	*alr3234*
hetP asl1930 alr2902				0.03
hetP asl1930 alr3234			N/A	
hetP alr2902 alr3234		-0.06		
asl1930 alr2902 alr3234	0.54			

The fitness of each mutant was defined as the difference in heterocyst percentage between the mutant and wild type counted at the time of maximal production after nitrogen stepdown, either 24 or 72 h. The heterocyst fitness of each mutant was used to calculate the epistatic interaction between loci. Gene combinations resulting in values less than 0 are interpreted as being synergistic, greater than 0 as antagonistic, and equal to zero as simply additive. N/A denotes the impossibility of the calculation because one of the strains did not produce heterocysts.

Table S3. Heterocyst production in strains overexpressing *hetP*, *asl1930*, *alr2902*, or *alr3234*.

Strain	Heterocyst Percentage after Nitrogen Stepdown					
	0 h	**24 h**	**48 h**	**72 h**	**96 h**	**120 h**
Wild type + P_{petE}	0.6 ± 0.72	8.1 ± 0.81	7.7 ± 0.81	7.7 ± 0.90	6.9 ± 0.83	7.2 ± 1.3
Wild type + P_{petE}-*hetP*	7.4 ± 1.0	14.6 ± 1.3	18.8 ± 1.6	21.6 ± 1.8	21.9 ± 2.3	18.5 ± 0.83
Wild type + P_{petE}-*asl1930*	0.3 ± 0.42	3.3 ± 0.81	6.1 ± 0.42	7.9 ± 0.99	7.4 ± 0.80	7.2 ± 0.72
Wild type + P_{petE}-*alr2902*	0.2 ± 0.20	8.1 ± 0.61	7.3 ± 1.2	7.5 ± 0.81	6.9 ± 0.50	7.0 ± 0.72
Wild type + P_{petE}-*alr3234*	0.4 ± 0.40	8.5 ± 0.50	7.8 ± 0.87	7.2 ± 1.1	6.9 ± 0.50	7.1 ± 0.42
Δ*hetR* + P_{petE}	0	0	0	0	0	0
Δ*hetR* + P_{petE}-*hetP*	0	0.2 ± 0.20	1.0 ± 0.20	4.7 ± 1.0	10.6 ± 1.4	43.9 ± 2.3
Δ*hetR* + P_{petE}-*asl1930*	0	0	0	0	0	0
Δ*hetR* + P_{petE}-*alr2902*	0	0	0	0	0	0
Δ*hetR* + P_{petE}-*alr3234*	0	0	0	0	0	0
Δ*hetP* + P_{petE}	0	0.3 ± 0.31	2.1 ± 0.31	2.8 ± 0.80	2.9 ± 0.42	2.3 ± 0.42
Δ*hetP* + P_{petE}-*hetP*	5.5 ± 0.81	12.8 ± 0.87	15.0 ± 1.3	18.8 ± 1.3	17.6 ± 1.3	17.7 ± 1.4
Δ*hetP* + P_{petE}-*asl1930*	0	0.2 ± 0.20	2.3 ± 0.42	2.5 ± 0.70	3.1 ± 0.61	2.6 ± 0.42
Δ*hetP* + P_{petE}-*alr2902*	0	4.0 ± 0.60	6.1 ± 0.70	6.7 ± 0.95	6.9 ± 0.31	6.9 ± 0.50
Δ*hetP* + P_{petE}-*alr3234*	0	0.2 ± 0.20	2.0 ± 0.53	3.1 ± 0.53	3.1 ± 0.95	3.2 ± 0.20
UHM333 + P_{petE}	0	0.4 ± 0.35	4.9 ± 0.95	7.0 ± 0.92	6.5 ± 0.70	6.7 ± 0.42
UHM333 + P_{petE}-*hetP*	6.7 ± 1.0	13.1 ± 2.1	13.7 ± 1.1	16.7 ± 1.2	16.9 ± 1.3	17.5 ± 2.0
UHM333 + P_{petE}-*asl1930*	0	5.7 ± 0.70	6.7 ± 0.64	8.1 ± 0.76	7.5 ± 1.2	8.6 ± 0.80
UHM333 + P_{petE}-*alr2902*	0	3.5 ± 1.3	6.5 ± 0.50	7.7 ± 0.90	7.7 ± 0.70	7.5 ± 0.31
UHM333 + P_{petE}-*alr3234*	0	0.5 ± 0.31	4.5 ± 0.99	6.8 ± 0.87	6.9 ± 0.81	7.3 ± 0.31

Heterocyst percentage produced by various strains individually complemented with *hetP*, *asl1930*, *alr2902*, or *alr3234* controlled by the *petE* promoter following the removal of combined nitrogen. At the indicated times following nitrogen stepdown, 500 cells were counted

in triplicate and total heterocysts are presented as the mean ± the standard deviation. Expression of the *petE* promoter was achieved by the addition of copper to a final concentration of 2 μM carried by the negative control plasmid (pPJAV213) or driving expression of *hetP* (pSMC224), *asl1930* (pKH282), *alr2902* (pKH281), or *alr3234* (pSMC226) in the wild type, Δ*hetR* (UHM103), Δ*hetP* (UHM158), or the quadruple homolog mutant (UHM333).

Table S4. BACTH protein interactions for HetR, HetP, Asl1930, Alr2902, and Alr3234.

Plasmid 1	Plasmid 2	Blue Color (Y/N)	Beta-gal Activity (MU±SD)
pT18-C-link	pT25-C-link	N	132.4 ± 22.4
pT18-N-link	pT25-C-link	N	154.8±36.5
pT18-C-link	pT25-N-link	N	148.4±15.3
pT18-N-link	pT25-N-link	N	163.7±33.3
pJP41: pUT18-divIVA	pJP42: pKNT25-divIVA	Y	6360.3±110.1
pRO176: T18C-hetP	pRO178: T25C-hetP	N	ND
pRO177: T18N-hetP	pRO178: T25C-hetP	N	ND
pRO180: T18C-asl1930	pRO178: T25C-hetP	N	ND
pRO181: T18N-asl1930	pRO178: T25C-hetP	N	ND
pRO184: T18Calr-2902	pRO178: T25C-hetP	N	ND
pRO185: T18N-alr2902	pRO178: T25C-hetP	N	ND
pRO188: T18C-alr3234	pRO178: T25C-hetP	N	ND
pRO189: T18N-alr3234	pRO178: T25C-hetP	N	ND
pST565: T18C-hetR	pRO178: T25C-hetP	N	ND
pST579: T18N-hetR	pRO178: T25C-hetP	N	ND
pRO176: T18C-hetP	pRO170: T25N-hetP	N	ND
pRO177: T18N-hetP	pRO170: T25N-hetP	N	ND
pRO180: T18C-asl1930	pRO170: T25N-hetP	N	ND
pRO181: T18N-asl1930	pRO170: T25N-hetP	Y	399.0±110.7
pRO184: T18Calr-2902	pRO170: T25N-hetP	N	ND
pRO185: T18N-alr2902	pRO170: T25N-hetP	N	ND
pRO188: T18C-alr3234	pRO170: T25N-hetP	N	ND
pRO189: T18N-alr3234	pRO170: T25N-hetP	Y	472.3±91.4
pST565: T18C-hetR	pRO170: T25N-hetP	N	ND
pST579: T18N-hetR	pRO170: T25N-hetP	N	ND
pRO176: T18C-hetP	pRO182: T25C-asl1930	N	ND
pRO177: T18N-hetP	pRO182: T25C-asl1930	N	ND
pRO180: T18C-asl1930	pRO182: T25C-asl1930	N	ND
pRO181: T18N-asl1930	pRO182: T25C-asl1930	N	ND
pRO184: T18Calr-2902	pRO182: T25C-asl1930	N	ND

pRO185: T18N-alr2902	pRO182: T25C-asl1930	N	ND
pRO188: T18C-alr3234	pRO182: T25C-asl1930	N	ND
pRO189: T18N-alr3234	pRO182: T25C-asl1930	Y	531.9±130.5
pST565: T18C-hetR	pRO182: T25C-asl1930	N	ND
pST579: T18N-hetR	pRO182: T25C-asl1930	N	ND
pRO176: T18C-hetP	pRO183: T25C-asl1930	N	ND
pRO177: T18N-hetP	pRO183: T25C-asl1930	N	ND
pRO180: T18C-asl1930	pRO183: T25C-asl1930	Y	262.3±28.6
pRO181: T18N-asl1930	pRO183: T25C-asl1930	N	ND
pRO184: T18Calr-2902	pRO183: T25C-asl1930	N	ND
pRO185: T18N-alr2902	pRO183: T25C-asl1930	Y	513.5±14.5
pRO188: T18C-alr3234	pRO183: T25C-asl1930	N	ND
pRO189: T18N-alr3234	pRO183: T25C-asl1930	N	ND
pST565: T18C-hetR	pRO183: T25C-asl1930	Y	376.2±63.5
pST579: T18N-hetR	pRO183: T25C-asl1930	N	ND
pRO176: T18C-hetP	pRO186: T25C-alr2902	N	ND
pRO177: T18N-hetP	pRO186: T25C-alr2902	N	ND
pRO180: T18C-asl1930	pRO186: T25C-alr2902	N	ND
pRO181: T18N-asl1930	pRO186: T25C-alr2902	N	ND
pRO184: T18Calr-2902	pRO186: T25C-alr2902	N	ND
pRO185: T18N-alr2902	pRO186: T25C-alr2902	N	ND
pRO188: T18C-alr3234	pRO186: T25C-alr2902	N	ND
pRO189: T18N-alr3234	pRO186: T25C-alr2902	Y	287.3±65.1
pST565: T18C-hetR	pRO186: T25C-alr2902	N	ND
pST579: T18N-hetR	pRO186: T25C-alr2902	N	ND
pRO176: T18C-hetP	pRO187: T25N-alr2902	N	ND
pRO177: T18N-hetP	pRO187: T25N-alr2902	Y	305.6±79.3
pRO180: T18C-asl1930	pRO187: T25N-alr2902	N	ND
pRO181: T18N-asl1930	pRO187: T25N-alr2902	Y	275.2±60.2
pRO184: T18C-alr-2902	pRO187: T25N-alr2902	Y	489.6±75.9
pRO185: T18N-alr2902	pRO187: T25N-alr2902	N	ND
pRO188: T18C-alr3234	pRO187: T25N-alr2902	N	ND
pRO189: T18N-alr3234	pRO187: T25N-alr2902	N	ND

pST565: T18C-hetR	pRO187: T25N-alr2902	Y	4899.3±1263.9
pST579: T18N-hetR	pRO187: T25N-alr2902	N	ND
pRO176: T18C-hetP	pRO190: T25C-alr3234	N	ND
pRO177: T18N-hetP	pRO190: T25C-alr3234	N	ND
pRO180: T18C-asl1930	pRO190: T25C-alr3234	N	ND
pRO181: T18N-asl1930	pRO190: T25C-alr3234	N	ND
pRO184: T18C-alr-2902	pRO190: T25C-alr3234	N	ND
pRO185: T18N-alr2902	pRO190: T25C-alr3234	Y	4676.8±361.8
pRO188: T18C-alr3234	pRO190: T25C-alr3234	N	ND
pRO189: T18N-alr3234	pRO190: T25C-alr3234	N	ND
pST565: T18C-hetR	pRO190: T25C-alr3234	N	ND
pST579: T18N-hetR	pRO190: T25C-alr3234	N	ND
pRO176: T18C-hetP	pRO191: T25N-alr3234	N	ND
pRO177: T18N-hetP	pRO191: T25N-alr3234	N	ND
pRO180: T18C-asl1930	pRO191: T25N-alr3234	Y	3209.5±506.9
pRO181: T18N-asl1930	pRO191: T25N-alr3234	N	ND
pRO184: T18C-alr-2902	pRO191: T25N-alr3234	Y	320.1±15.3
pRO185: T18N-alr2902	pRO191: T25N-alr3234	N	ND
pRO188: T18C-alr3234	pRO191: T25N-alr3234	N	ND
pRO189: T18N-alr3234	pRO191: T25N-alr3234	Y	6034.1±414.0
pST565: T18C-hetR	pRO191: T25N-alr3234	N	ND
pST579: T18N-hetR	pRO191: T25N-alr3234	N	ND
pRO176: T18C-hetP	pST558: T25C-hetR	N	ND
pRO177: T18N-hetP	pST558: T25C-hetR	N	ND
pRO180: T18C-asl1930	pST558: T25C-hetR	N	ND
pRO181: T18N-asl1930	pST558: T25C-hetR	N	ND
pRO184: T18C-alr-2902	pST558: T25C-hetR	N	ND
pRO185: T18N-alr2902	pST558: T25C-hetR	N	ND
pRO188: T18C-alr3234	pST558: T25C-hetR	N	ND
pRO189: T18N-alr3234	pST558: T25C-hetR	Y	5715.0±639.9
pST565: T18C-hetR	pST558: T25C-hetR	Y	8823.4±2490.2
pST579: T18N-hetR	pST558: T25C-hetR	Y	9114.8±1821.9
pRO176: T18C-hetP	pST572: T25N-hetR	N	ND

pRO177: T18N-hetP	pST572: T25N-hetR	N	ND
pRO180: T18C-asl1930	pST572: T25N-hetR	N	ND
pRO181: T18N-asl1930	pST572: T25N-hetR	N	ND
pRO184: T18C-alr-2902	pST572: T25N-hetR	N	ND
pRO185: T18N-alr2902	pST572: T25N-hetR	N	ND
pRO188: T18C-alr3234	pST572: T25N-hetR	N	ND
pRO189: T18N-alr3234	pST572: T25N-hetR	Y	324.5±15.4
pST565: T18C-hetR	pST572: T25N-hetR	Y	4689.4±1001.7
pST579: T18N-hetR	pST572: T25N-hetR	Y	2818.2±942.1

Blue color: A blue color was detected when grown on solid media supplemented with X-gal
Beta-gal activity: Average miller units (MU) and standard deviation (SD) of three replicates
ND: Not determined

Table S5. Strains and plasmids used in this study.

Strain	**Relevant characteristics***	**Source**
PCC 7120	Wild type	Pasteur Culture Collection
UHM103	Δ*hetR*	(1)
UHM158	Δ*hetP*	(2)
UHM101	Δ*patA*	(3)
UHM334	Δ*patS*::Ω Sp^r/Sm^r	(4)
UHM288	Δ*hetP* Δ*asl1930*	This study
UHM287	Δ*hetP* Δ*alr2902*	This study
UHM286	Δ*hetP* Δ*alr3234*	This study
UHM223	Δ*hetP* Δ*patS*::Ω Sp^r/Sm^r	This study
UHM282	Δ*hetP* Δ*asl1930* Δ*alr2902*	This study
UHM283	Δ*hetP* Δ*asl1930* Δ*alr3234*	This study
UHM284	Δ*hetP* Δ*alr2902* Δ*alr3234*	This study
UHM333	Δ*hetP* Δ*asl1930* Δ*alr2902* Δ*alr3234*	This study
UHM295	Δ*asl1930*	This study
UHM340	Δ*alr2902*	This study
UHM336	Δ*alr3234*	This study
UHM297	Δ*asl1930* Δ*alr2902*	This study
UHM341	Δ*asl1930* Δ*alr3234*	This study
UHM343	Δ*alr2902* Δ*alr3234*	This study
UHM342	Δ*asl1930* Δ*alr2902* Δ*alr3234*	This study
Plasmid		
pAM504	Shuttle vector for replication in *E. coli* and *Anabaena*; Km^r Nm^r	(5)
pAM1951	pAM504 carrying P_{patS}-*gfp*	(6)
pAM1956	Shuttle vector pAM504 with promoterless *gfp*	(6)
pRL277	Suicide vector; Sp^r/Sm^r	(7)
pSMC164	Suicide plasmid used to replace *patS* with Sp^r/Sm^r Ω interposon	(8)
pSMC224	Shuttle vector carrying P_{petE}-*hetP*	(2)
pKH282	Shuttle vector carrying P_{petE}-*asl1930*	(2)
pKH281	Shuttle vector carrying P_{petE}-*alr2902*	(2)
pSMC226	Shuttle vector carrying P_{petE}-*alr3234*	(2)
pPJAV213	pAM504 carrying P_{petE}	(9)
pT18-N-link	Vector harboring the T18 domain of adenylate cyclase with a flexible linker region for N-terminal fusions; Ap^r	Gift from Dan Kearns, Indiana University
pT18-C-link	Vector harboring the T18 domain of adenylate cyclase with a flexible linker region for C-terminal fusions; Ap^r	Gift from Dan Kearns, Indiana University
pT25-N-link	Vector harboring the T25 domain of adenylate cyclase with a flexible linker region for N-terminal fusions; Km^r	Gift from Dan Kearns, Indiana University
pT25-C-link	Vector harboring the T25 domain of adenylate cyclase with a flexible linker region for C-terminal fusions; Km^r	Gift from Dan Kearns, Indiana University

pJP41	pUT18 carrying *divIVA* from *Bacillus subtilis*	(10)
pJP42	pKNT25 carrying *divIVA* from *Bacillus subtilis*	(10)
pST558	pKT25 carrying *hetR*	(11)
pST565	pUT18C carrying *hetR*	(11)
pST572	pKNT25 carrying *hetR*	(11)
pST579	pUT18 carrying *hetR*	(11)
pKH239	pRL277 used to delete *alr2902*	This study
pKH241	pRL277 used to delete *alr3234*	This study
pKH274	pRL277 used to delete *asl1930*	This study
pPJAV298	pAM504 carrying P_{hetP}-*hetP*(25aa)	This study
pPJAV299	pAM504 carrying P_{hetP}-*hetP*(50aa)	This study
pPJAV300	pAM504 carrying P_{hetP}-*hetP*(68aa)	This study
pPJAV301	pAM504 carrying P_{hetP}-*hetP*(75aa)	This study
pPJAV302	pAM504 carrying P_{hetP}-*hetP*(100aa)	This study
pPJAV303	pAM504 carrying P_{hetP}-*hetP*(125aa)	This study
pPJAV304	pAM504 carrying P_{hetP}-*hetP*	This study
pPJAV305	pAM504 carrying P_{hetP}-*hetP*(C36A)	This study
pPJAV306	pAM504 carrying P_{hetP}-*hetP*(C95A)	This study
pPJAV307	pAM504 carrying P_{hetP}-*hetP*(C36A, C95A)	This study
pPJAV327	pRL277 to reintroduce *hetP* at the native locus	This study
pPJAV330	pAM504 carrying $P_{asl1930}$-*gfp*	This study
pPJAV331	pAM504 carrying $P_{alr2902}$-*gfp*	This study
pPJAV332	pAM504 carrying $P_{alr3234}$-*gfp*	This study
pPJAV353	pAM504 carrying P_{hetP}-*asl1930*(68aa)	This study
pPJAV354	pAM504 carrying P_{hetP}-*alr2902*(68aa)	This study
pPJAV358	pAM504 carrying P_{hetP}-*alr3234*(68aa)	This study
pRO176	pT18-C-link carrying C-terminal *hetP* T18 fusion	This study
pRO177	pT18-N-link carrying N-terminal *hetP* T18 fusion	This study
pRO178	pT25-C-link carrying C-terminal *hetP* T25 fusion	This study
pRO179	pT25-N-link carrying N-terminal *hetP* T25 fusion	This study
pRO180	pT18-C-link carrying C-terminal *asl1930* T18 fusion	This study
pRO181	pT18-N-link carrying N-terminal *asl1930* T18 fusion	This study
pRO182	pT25-C-link carrying C-terminal *asl1930* T25 fusion	This study
pRO183	pT25-N-link carrying N-terminal *asl1930* T25 fusion	This study
pRO184	pT18-C-link carrying C-terminal *alr2902* T18 fusion	This study
pRO185	pT18-N-link carrying N-terminal *alr2902* T18 fusion	This study
pRO186	pT25-C-link carrying C-terminal *alr2902* T25 fusion	This study
pRO187	pT25-N-link carrying N-terminal *alr2902* T25 fusion	This study
pRO188	pT18-C-link carrying C-terminal *alr3234* T18 fusion	This study
pRO189	pT18-N-link carrying N-terminal *alr3234* T18 fusion	This study
pRO190	pT25-C-link carrying C-terminal *alr3234* T25 fusion	This study
pRO191	pT25-N-link carrying N-terminal *alr3234* T25 fusion	This study

*Ap, ampicillin, Km, kanamycin; Nm, neomycin; Sp, spectinomycin; Sm, streptomycin

Table S6. Oligonucleotide primers used in this study.

Oligonucleotide*	**Sequence**
1930-up-F	ATATAAGATCTATCGGGATGGTTTAACTCTC
1930-up-R	TTCCATCATCCCGGGAAAGATTCTTGAGTCATCAGC
1930-dn-F	CAAGAATCTTTCCCGGGATGATGGAATTAGATTAAAG
1930-dn-R	ATATAGAGCTCAAGAACTACAACAATCTGC
d2902-up-F	ATATAAGATCTAGTGATTCTTCATCTCCCTC
d2902-up-R	TTTTCCGATACCCGGGTAGCTCATAGTGTCTTGGAG
d2902-dn-F	CTATGAGCTACCCGGGTATCGGAAAAAGCTAGGTTC
d2902-dn-R	ATATAGAGCTCATAACTGTCCTAGAGATAGC
d3234-up-F	ATATAAGATCTAACTCAAGGAAACGATAGTC
d3234-up-R	TCAAATCAAGCCCGGGCATCCAGCTAACATCAAACC
d3234-dn-F	TAGCTGGATGCCCGGGCTTGATTTGAACCACATCTG
d3234-dn-R	ATATAGAGCTCTTTCGATTAAGCGAACATCG
hetP-up-XhoI	ATATACTCGAGTTGTCTAGTCAGTTGTCAGTCGTCAATAG
hetP-25aa-EcoRV-R	GAAGTCACATCAGATATCTCATTCAACCACTTTGTCAAATTGTTGAGGATTG
hetP-50aa-EcoRV-R	GAAGTCACATCAGATATCTCAGTAGTGCATAGGATTGTACCCAGCAAAGCG
hetP-68aa-EcoRV-R	GAAGTCACATCAGATATCTCATTTGCTAGCTTCGGAGTTTTCTTTGAG
hetP-75aa-EcoRV-R	GAAGTCACATCAGATATCTCAATCGTGTTGTTGTTGCTGTACTTTGC
hetP-100aa-EcoRV-R	GAAGTCACATCAGATATCTCAGATTTTACTTAAGCAACTGGACGGC
hetP-125aa-EcoRV-R	GAAGTCACATCAGATATCTCATAACCATTGATCTAAATTACCACCATG
hetP-159aa-EcoRV-R	GAAGTCACATCAGATATCTCAATTATGAATAAAATCTAGGTCTGACAGTTTG
hetPC36A-F M475L	AAATACTCTTGGGCTGCTGTTCTCATGCTGCG
hetPC36A-R M475L	CGCAGCATGAGAACAGCAGCCCAAGAGTCTTT
hetPC95A-F M475L	AATATGCCGTCCAGTGCCTTAAGTAAAATCAA
hetPC95A-R M475L	TTGATTTTACTTAAGGCACTGGACGGCATATT
Pasl1930-XhoI-F M475L	ATATACTCGAGTCTATTACAATGGCTCGTTGAAAAGTGTTCTGGC
Pasl1930-R M475L	CAGCCTAAATTATAAACGTGAATTTAAATGTTGAG
Palr2902-XhoI-F M475L	ATATACTCGAGTAGGTAACTGTTTTGCGATAAATTTTTTGTCTGTG
Palr2902-R M475L	AGTGTCTTGGAGATATTTATCTAAATATGAAATTTATAGACTG

Palr3234-XhoI-F M475L	ATATACTCGAGTCATACTTGGGCAGTTACAGTCACAGGCG
Palr3234-R M475L	CAAACCCTGATAAAACAAGACTTTCAAATCTGTCAACAGTC
PhetP-R	GGTTGTTATTGTTTTGGATGAAAATATCTCAGC
asl1930-68aa-F	TCCAAAACAATAACAACCATGACTCAAGAATCTTTCCAGCATCATCAAC
asl1930-68aa-R	TCATGTATCTGGCATACTATTATTTTTGAGTAGGCG
alr2902-68aa-F	TCCAAAACAATAACAACCATGAGCTACCACATAAATTCTTCCCAAAATCGG
alr2902-68aa-R	TCAATTGGCAACTTGTCTATTGTCCTTC
alr3234-68aa-F	TCCAAAACAATAACAACCATGTATCAGGAAGACATTTACAATTCACAG
alr3234-68aa-R	TCATTTCCCACCCAGACAGTTGTTTTTGAG
del-hetP-up-F	TATATAGATCTGAATAGAGTATGGAGAAGC
del-hetP-dn-R	TATATGAGCTCAAGCGAATTGCGTTTTGCG
del-hetP-up-out	ATAACGGGTGACATTCATG
del-hetP-dn-out	TGTCTTCCAAAGTTCAGATGC
1930-up-out	GAAGAATCAGATGGGACTTGGGC
1930-dn-out	CCCAGAAAATCATTGCTGATACTGCT
2902-up-out	ATCTGTCTTTGCTACGCAAC
2902-dn-out	TCCAATAACTTACCCACGAC
3234-up-out	ACAATTACTAAAGCGACTGC
3234-dn-out	ATAAGTTTTGGGTGGTACTG
patSfor	GATATCTAATCGATGCCACATCTAAG
patSrev	CACATTAATCTCACTAACTTCTACATC
Bac2-N-asl1930 XbaI F	AGGAGTCTAGAGACTCAAGAATCTTTCCAGCATCATC
Bac2-N-asl1930 KpnI R	CTCCTGGTACCCGATCTAATTCCATCATCTTTATTTTAATAG
Bac2-C-asl1930 XbaI F	AGGAGTCTAGAACTCAAGAATCTTTCCAGCATCATC
Bac2-C-asl1930 KpnI R	CTCCTGGTACCATCTAATTCCATCATCTTTATTTTAATAG
Bac2-N-alr2902 XbaI F	AGGAGTCTAGAGAGCTACCACATAAATTCTTCCCAAAA
Bac2-N- alr2902 KpnI R	CTCCTGGTACCCGTTGATTCCGGCTATACATTACTGCC
Bac2-C- alr2902 XbaI F	AGGAGTCTAGAAGCTACCACATAAATTCTTCCCAAAA
Bac2-C- alr2902 KpnI R	CTCCTGGTACCTTGATTCCGGCTATACATTACTGCC
Bac2-N-alr3234 XbaI F	AGGAGTCTAGAGTTAGCTGGATGTTTTAATCTATCTGG
Bac2-N- alr3234 KpnI R	CTCCTGGTACCCGAATCAAGACCTCTTGAGAGTCATTTC
Bac2-C- alr3234 XbaI F	AGGAGTCTAGATTAGCTGGATGTTTTAATCTATCTGG

Bac2-C- alr3234 KpnI R	CTCCTGGTACCAATCAAGACCTCTTGAGAGTCATTTC
Bac2-N-hetP XbaI F	AGGAGTCTAGAGAACCAAAACACTACAGGCATAACCA
Bac2-N- hetP KpnI R	CTCCTGGTACCCGATTATGAATAAAATCTAGGTCTGACAG
Bac2-C- hetP XbaI F	AGGAGTCTAGAAACCAAAACACTACAGGCATAACCA
Bac2-C- hetP KpnI R	CTCCTGGTACCATTATGAATAAAATCTAGGTCTGACAG
T25N-NheI F	AGGAGGCTAGCGCCCAATACGCAAACCGCCTCTCCCC
T25N-link-EcoRI R	CTCCTGAATTCGAGCCAGAACCAGCAGCGGAGCCAGCGGAACCGCTCGGTACC CGGGGATCCTCTAGA
T25C-HindIII F	AGGAGAAGCTTTAATGCGGTAGTTTATCACAGTT
T25C-link-PstI R	CTCCTCTGCAGCCAGAACCAGCAGCGGAGCCAGCGGAACCCGCCCGCCGCGTG CGCGCCAG
T18N-link-EcoRI F	AGGAGGAATTCGGGTTCCGCTGGCTCCGCTGCTGGTTCTGGCGGAGCCGCCAG CGAGGCCACGGGC
T18N-EagI R	CTCCTCGGCCGCCGCAATCCGGGTGACGCCGGCAC
T18C-HindIII F	AGGAGAAGCTTAGCCGCCAGCGAGGCCACG
T18C-link-PstI R	CTCCTCTGCAGGCCAGAACCAGCAGCGGAGCCAGCGGAACCGTGGCGTTCCAC TGCGCCCAGCGACGG
NrnpAF	TACGCTCATTGGTGTCTCG
NrnpAR	AACAACTGCTCTAATTCTTGC
asl1930-qF	TGACTCAAGAATCTTTCCAGCA
asl1930-qR	AGCCCAAGAATACTTACCGACA
alr2902-qF	TCTTCCCAAAATCGGTTTCACA
alr2902-qR	CGGCTATAAGTCCGTTGGGG
alr3234-qF	TCAGGGGAAGTTATGTATCAGGA
alr3234-qR	GCAGTAAAACGCAAGCCCAA
hetP-qF	TGCACTACATTCCCTACCGC
hetP-qR	ACTTAAGCAACTGGACGGCAT

*Oligonucleotides are shown in the 5’ to 3’ direction.